# Uncommon overoxidative catalytic activity in a new halo-tolerant alcohol dehydrogenase

Martina L. Contente,[a] Noemi Fiore, [b] Pietro Cannazza,[b] David Roura-Padrosa,[c] Francesco Molinari,[b]* Louise Gourlay, [d] Francesca Paradisi [a,c]*

Dedication ((optional))

[a] Dr. M. L. Contente, Prof. F. Paradisi
School of Chemistry
University of Nottingham
University Park, Nottingham, NG7 2RD, UK

[b] N. Fiore, P. Cannazza, Prof. F. Molinari
Department of Food, Environmental and Nutritional Sciences (DeFENS)
University of Milan
via Mangiagalli 25, 20133 Milan, Italy
E-mail: francesco.molinari@unimi.it

[c] Dr. D. Roura Padrosa, Prof. F. Paradisi
Department of Chemistry and Biochemistry
University of Bern
Freiestrasse 3, 3012 Bern, Switzerland
E-mail: francesca.paradisi@dcb.unibe.ch

[d] Dr. Louise Gourlay
Department of Biosciences (DBS),
University of Milan
via via Celoria 26, 20133 Milan, Italy

Supporting information for this article is given via a link at the end of the document.((Please delete this text if not appropriate))

**Abstract:** Alcohol dehydrogenases (ADH) are versatile and useful enzymes employed as biocatalysts, especially for the selective oxidation of primary and secondary alcohols, and for the reduction of carbonyl moieties. A new alcohol dehydrogenase (HeADH-II) has been identified from the genome of the halo-adapted bacterium *Halomonas elongata*, which proved stable in the presence of polar organic solvents and salt exposure. Unusual for this class of enzymes, HeADH-II lacks enantiopreference and is capable of oxidizing both alcohols and aldehydes, enabling a direct overoxidation of primary alcohols to carboxylic acids. HeADH-II was coupled with a NADH-oxidase from *Lactobacillus pentosus* (*Lp*NOX) to increase the process yields and allowing recycling of the cofactor. The enzymatic oxidation of primary alcohols was also paired with *in situ* condensation of the intermediate aldehydes with hydroxylamine to prepare the corresponding aldoximes, with particular attention to perillartine (a powerful sweetener), whose enzymatic synthesis starting from natural sources, leads to an equally natural product. Analysis of the apo-crystal structure of HeADH-II (4.0 Å), highlighted evident active sites similarities with two mammalian ADHs that also have overoxidative activities, implying possible shared catalytic mechanisms.

## Introduction

Alcohol dehydrogenases (ADHs) have acquired increasing interest as versatile chemo- and enantioselective biocatalysts.[1-3] While classic ADH-mediated oxidation of alcohols to the corresponding carbonyl compounds are well known,[4-6] just a few examples of complete (primary) alcohol oxidation to carboxylic acids have been reported to date, often involving complex cascade enzymatic reactions.[7-9] The identification of novel biocatalysts capable of overoxidative activity towards primary alcohols under mild conditions is essential for green and sustainable chemistry.[8] Classically, the oxidation of primary alcohols is chemoselective and leads to the exclusive formation of aldehydes. Further oxidation is generally obtained by coupling ADHs with an aldehyde dehydrogenase (AldDH) or by using whole cell systems, such as acetic acid bacteria.[10,11] However, oxidation of aldehydes *via* ADH has been observed with horse liver dehydrogenase (HLADH), which catalyzes the dismutation of short-chain aliphatic aldehydes, in the presence of an excess of $NAD^+$;[6] the complex HLADH-$NAD^+$ firstly performs the oxidation of the aldehyde generating the carboxylic acid, while the newly formed complex (HLADH-NADH) binds another aldehyde molecule, catalyzing its reduction to alcohol. In this fine equilibrium, the hydration of the aldehyde plays an important role since the free form is the substrate for reduction, whereas the hydrate *gem*-diol is the actual substrate for oxidation. With simple aliphatic aldehydes, which freely interconvert between the two forms, an equivalent amount of alcohols and carboxylic acids is formed at the end of the process with HLADH, thus promoting an enzymatic Cannizzaro reaction.[7] Könst *et al.* screened 70 different ADHs and only 9 showed significant accumulation of acid, demonstrating that this activity is rather an exception.[9] In particular, a mutant ADH (ADH-9V1), with lower binding affinity towards NADH than the wild-type enzyme, was

able to better catalyze aldehyde oxidation. The conversion was further increased by recycling the cofactor with an $H_2O$-forming NAD(P)H-oxidase (NOX) from *Lactobacillus sanfranciscensis* and performing the reaction at pH 9.0 where a higher amount of *gem*-diol is present. Under optimized conditions (21 h), ADH-9V1 catalyzed the oxidation of primary alcohols into carboxylic acids with conversions ranging from 9 to 37% for aromatic substrates, and 70-73% for simple aliphatic alcohols.[9]

New enzymes with improved solvent tolerance may be found in extremophiles.[12] ADHs with greater stability towards polar organic solvents have been expressed from halophilic microorganisms[13] and from amplified genomes from unculturable species occurring in brine pool.[14,15] In this work, an ADH gene (HeADH-II) identified from the genome of *Halomonas elongata* was codon optimized and expressed in *E. coli*; *Halomonas elongata* is a halo-adapted bacterium which has been previously used as source of enzymes with remarkable solvent-tolerance and stability under operating conditions.[16-19] HeADH-II was characterized and used as biocatalyst, proving its ability to oxidize both primary alcohols and aldehydes, showing enhanced stability towards water-miscible co-solvents (*e.g.,* DMSO).

In order to gain insight into the possible structural determinants of the overoxidative activities of HeADH-II, the low-resolution crystal structure of the apo-form of HeADH-II, solved at 4.0 Å, is here-presented, revealing a tetrameric quaternary arrangement and the canonical monomeric fold of the zinc-dependent ADHs. Despite the resolution of the data, the coordinating residues of the zinc binding sites were visible, enabling us to infer structural similarities with other ADH enzymes of mammalian origin that also catalyze alcohol overoxidations.

## Results and Discussion

The activity and stability of HeADH-II were firstly evaluated using the reduction of cinnamaldehyde to cinnamyl alcohol as standard reaction (See Supporting Information). The highest activity of HeADH-II was found at pH 5.0 in a temperature range of 45-65 °C. The presence of salts has been well tolerated; the utmost activity was surprisingly recorded in the presence of 3 M NaCl; remarkably, the addition of DMSO had minor effect on the enzyme performance since only 8% of the original activity was lost in the presence of 10% (*v/v*) DMSO, and just 18% with 20% (*v/v*) of the same co-solvent. The highest stability was found at 25 °C and pH 8.0; high stability was also observed in the presence of NaCl and KCl and DMSO (10-20%), confirming the possibility of using HeADH-II with water-miscible co-solvents or relatively high salt concentrations.

Reduction of cinnamaldehyde (20 mM) into cinnamyl alcohol, with a stoichiometric amount of NADH, was carried out at pH 8.0, 30 °C (best compromise between activity and stability) in the presence of HeADH-II (1 U/mL), showing 65% molar conversion. Relatively high concentrations of DMSO (15%) were used to better solubilize cinnamaldehyde, which is only slightly soluble in water (1.05 g/L, 8 mM at 20 °C).[20]

The reverse reaction (oxidation of cinnamyl alcohol) was performed in the presence of stoichiometric amounts of $NAD^+$ at different pHs. Oxidation generally occurred with formation of cinnamaldehyde and, unexpectedly, cinnamic acid, albeit with low conversion of the substrate (Scheme 1). To increase the yields of the oxidations, bioconversions were carried out with HeADH-II (1 U/mL) in the presence of $NAD^+$ (0.1-10 mM), a NADH-oxidase from *Lactobacillus pentosus* (*Lp*NOX) (10 U/mL) and FAD (0.1 mM) (Scheme 1).

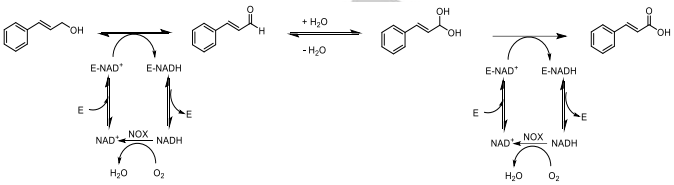


**Scheme 1.** Oxidation of cinnamyl alcohol and cinnamaldehyde with cofactor recycling

To combine the two different enzymes in an one-pot reaction, the reaction conditions were set so that also *Lp*NOX (employed to re-oxidize the cofactor) could optimally perform; *Lp*NOX is active between pH 5.0-9.0 and 25-50 °C.[21] Therefore, preparative oxidation of both cinnamyl alcohol and cinnamaldehyde were firstly carried out at different pHs (5.0-8.0) and 30 °C. The reaction leads to the accumulation of aldehyde, as also seen in the experiments without cofactor regeneration with a maximum conversion around 93-95%, while cinnamic acid was produced only in small amounts. The biotransformation did not proceed further after the apparent equilibrium was reached within one hour, regardless of the medium pH. This behavior may be ascribed to the low stability of *Lp*NOX, with subsequent interruption of cofactor recycling. To check this hypothesis, fresh *Lp*NOX (10 U) was added after each hour, showing that oxidation proceeded to carboxylic acid with conversions up to 99% (See Supporting Information), again independently of the pH.

The oxidative reaction with fed-batch addition of *Lp*NOX was then applied to different aromatic alcohols and aldehyde (Table 1).

**Table 1.** Oxidation of different primary alcohols using HeADH-II.

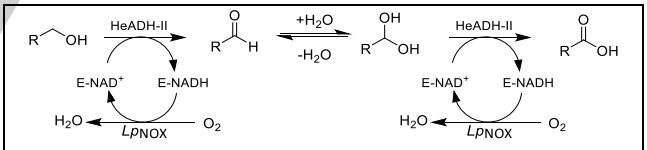


| Entry | Substrate | Aldehyde | Acid | Time (h) |
|---|---|---|---|---|
| 1 | Cinnamyl alcohol[a] | - | > 98 | 4 |
| 2 | Benzyl alcohol[a] | 10 | 90 | 16 |
| 3 | Piperonyl alcohol[a] | 5 | 95 | 16 |
| 4 | 4-Methoxybenzyl alcohol[a] | - | > 98 | 8 |
| 5 | 2-Phenyl-1-ethanol[b] | - | > 98 | 2 |
| 6 | 3-Phenyl-1-propanol[b] | - | > 98 | 2 |
| 7 | (*R,S*)-2-Phenyl-1-propanol[b] | - | > 98 | 3 |

Reaction conditions: a) 20 mM substrate in DMSO (15% *v/v*), 0.1 mM $NAD^+$, 0.1 mM FAD, HeADH-II (1 U/mL) in Tris-HCl buffer 100 mM, pH 8.0, fed-batch addition of *Lp*NOX (10 U) every hour; b) 20 mM substrate in DMSO (15% *v/v*), 0.1 mM $NAD^+$, 0.1 mM FAD, HeADH-II (1 U/mL), LpNOX (10 U/mL), in Tris-HCl buffer 100 mM, pH 8.0 at 30 °C.

The bioconversion of benzyl alcohol derivatives (Entries 2-4, Table 1) occurred in a manner similar to what was observed with cinnamyl alcohol, with an initial accumulation of aldehyde and complete oxidation into carboxylic acids with fed-batch addition of *Lp*NOX. For fast-reacting substrates (Entries 5-7, Table 1), acid formation was complete in short timescales without further

addition of *Lp*NOX. Surprisingly, despite the short reaction time, no trace of enantioselectivity was observed with racemic 2-phenyl-1-propanol (Entry 7), which was completely oxidized in 3 hours obtaining the corresponding acid as racemate. With respect to the previous reported methodology, involving a mutated ADH with lower affinity for NADH,[9] the new strategy allows a 4-fold higher substrate loading (20 mM) while the aromatic acids were obtained with greater yields and in shorter reaction times.

To further investigate the substrate scope of this new enzyme, secondary alcohols were also tested under the above described reaction conditions (Figure 1); no fed-batch addition of *Lp*Nox was necessary. Virtually all reported ADHs display a strong enantiopreference towards either *R* or *S* secondary alcohols,[22] but while HeADH-II showed activity towards (*R*,*S*)-1-phenyl ethanol (**1a**, Figure 1, 65% m.c., 2 h) no enantiopreference was observed. No conversion was obtained with the bulkier (*R*,*S*)-1-phenyl-2-propanol (**1b**, Figure 1).

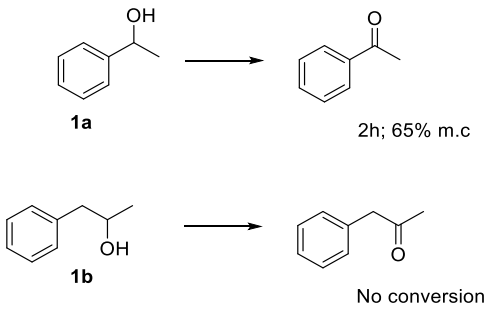


**Figure 1.** Oxidation of secondary alcohols using HeADH-II. Reaction conditions: 20 mM substrate in DMSO (15% *v/v*), 0.1 mM $NAD^+$, 0.1 FAD, HeADH-II (1 U/mL), *Lp*NOX (10 U/mL), in Tris-HCl buffer 100 mM, pH 8.0 at 30 °C.

To confirm the rare characteristic concerning the lack of enantioselectivity of the enzyme, HeADH-II was assayed also in the reductive direction with acetophenone (20 mM) and a stoichiometric amount of NADH. The corresponding racemic 1-phenyl ethanol was obtained as product (70% m.c., 6 h) (See Supporting information).

HeADH-II was subsequently employed for the direct oxidation of aldehydes into the corre-sponding carboxylic acids with high conversion (Table 2).

**Table2.** Oxidation of different aldehydes using HeADH-II.

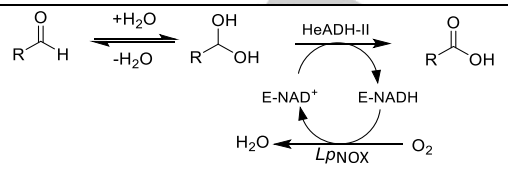


| Entry | Substrate | Acid (%) | Time (h) |
|---|---|---|---|
| 1 | Cinnamaldehyde | 94 | 6 |
| 2 | Benzaldehyde | > 98 | 8 |
| 3 | Piperonal | > 98 | 8 |
| 4 | 4-Methoxybenzaldehyde | > 98 | 8 |
| 5 | Phenylacetaldehyde | > 98 | 2 |
| 6 | 3-Phenylpropionaldehyde | > 98 | 2 |
| 7 | (*R*,*S*)-2-Phenylpropanal | >99 | 2 |

Reaction conditions: 20 mM substrate in DMSO (15% *v/v*), 0.1 mM $NAD^+$, 0.1 mM FAD, HeADH-II (1 U/mL), LpNOX (10 U/mL), in Tris-HCl buffer 100 mM, pH 8.0 at 30 °C.

Aldehyde oxidation was generally rapid, and no further addition of *Lp*NOX was necessary to obtain high yields in short reaction times. Transient formation of aldehydes in the two-step enzymatic oxidation of primary alcohols at pH 8.0 led us to explore the possibility of condensing the intermediate aldehydes with hydroxylamine, thus furnishing the corresponding aldoximes.[23] In this instance, three different substrates were selected (Table 3).

**Table3.** Oxidation of primary alcohols using HeADH-II in the presence of $NH_2OH$.

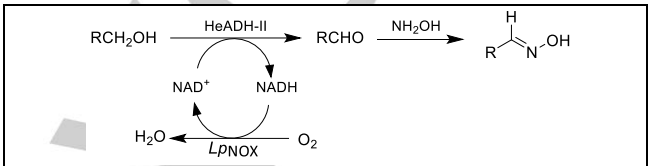


| Entry | Substrate | Aldoxime (%) | Time (h) |
|---|---|---|---|
| 1 | Cinnamyl alcohol | 86 | 3 |
| 2 | Benzyl alcohol | 86 | 6 |
| 3 | Perillyl alcohol | 82 | 2 |

Reaction conditions: 20 mM substrate in DMSO (15% *v/v*), $NH_2OH{\cdot}HCl$ (24 mM), 0.1 mM $NAD^+$, 0.1 mM FAD, HeADH-II (1 U/mL), *Lp*NOX (10 U/mL), in Tris-HCl buffer 100 mM, pH 8.0 at 30 °C.

The biotransformations performed in the presence of $NH_2OH$ allowed the recovery of the aldoximes with conversions >80%. It should be noted that aldoximes can be easily converted into aldehydes by mild and efficient hydrolysis. Synthesis of perillartine from perillyl alcohol (Entry 3, Table 3, Scheme 2) was investigated as a molecule of interest in the food industry. It is typically employed as non-protein sweetener since it is 2000-fold sweeter than sucrose. Perillartine is usually chemically prepared, starting from perillaldehyde extracted from plants (*e.g., Perilla frutescens*).[24] Particular attention to the synthesis of this compound was promoted by the need to develop natural processes for the preparation of food additives: the obtainment of perillartine through the enzymatic conversion of a natural substrate allows to label and commercialize the corresponding product as natural too, thus increasing its market value.

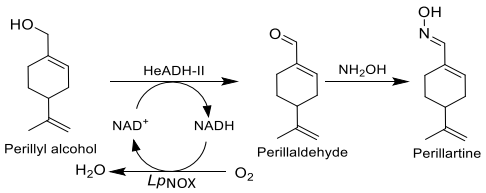


**Scheme 2.** Preparation of perillartine from perillyl alcohol

**The 3D structure of apo-HeADH-II**

In order to understand the structural arrangement of HeADH-II that may explain its peculiar overoxidative activities, the crystal structure of apo-HeADH-II was solved, as described in the Sup-porting information section. In agreement with size exclusion

chromatography studies (See Supporting Information), HeADH-II assembles as a compact tetramer with an estimated assembly ΔG of -137.5 kcal/mol, as calculated using PDBePISA[25] (https://www.ebi.ac.uk/msd-srv/prot_int/cgi-bin/piserver; Figure 1a). Electron density was present for main chain residues 2 to 341 (chain A), 4 to 341 (chain B) 6 to 332 (chain C) and 5 to 341 (chain D). The remaining N- and C-terminal residues and other loop regions were absent and lost to the solvent. Despite the low resolution of the data, the two zinc binding sites per chain were clearly observed (Figure 1b & Supporting Information Figure S8).

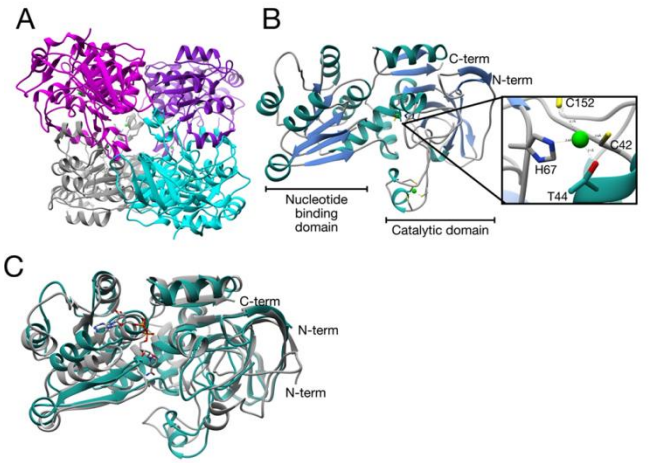


Figure 1. The crystal structure of HeADH-II. A) The quaternary arrangement of HeADH-II, illustrating the tetramer present in the crystal asymmetric unit; B) Secondary structure ribbon representation of the HeADH-II monomer, indicating the nucleotide binding domain, the catalytic domain, the N- and C-termini and bound zinc ions (green spheres). A close-up of the catalytic zinc binding site of chain B is shown with the coordinating residues in sticks; C) Superposition of chain A of HeADH-III (green) with human liver χχ ADH (grey) PDB entry 1TEH).[26] The bound NAD(H) cofactor of human liver χχ ADH is shown (sticks) to highlight the coenzyme binding site. This figure was prepared using Chimera.[27]

In line with other zinc-dependent ADHs, each apo-HeADH-II monomer folds into two sub-domains: a catalytic domain composed of a central mixed β-sheet, flanked by two antiparallel β-sheets, six α-helices and three 310 helices, and a smaller nucleotide-binding domain, which adopts the canonical Rossmann fold, typical of NAD(H)-binding proteins, comprising a six-stranded parallel β-sheet flanked by six α-helices (Figure 1b). A long helical hinge region (residues 144-165) connects the two domains, forming a cleft to which the coenzyme binds in other ADHs of known structure. Based on apo- and coenzyme bound structures, significant conformational changes are proposed to occur during the mechanism due to this hinge region, with the enzyme alternating be-tween an open, unbound form to a closed, coenzyme and substrate-bound form.[28]

In agreement with our functional data showing that HeADH-II efficiently catalyzes the oxidation of cinnamyl alcohol, the DALI secondary structure matching server (http://ekhidna2.biocenter.helsinki.fi/dali/),[29] revealed the cinnamyl ADH (SbCAD4; PDB entry 5VKT) from *Sorghum bicolor* (RMSD 2.1Å over 333/353 aligned C-alpha atoms; 31% sequence identity) as the top structural homolog.[30] The main structural differences arise in loop regions and in the catalytic domain, and also in the overall quaternary arrangement, with SbCAD4, being a dimer. Both HeADH-II and cinnamyl ADHs are zinc-dependent enzymes, however the latter prefers NADP(H) to NAD(H) and usually favors aldehyde reduction over alcohol oxidation.[30]

**The He-ADH-II active site**

Each HeADH-II chain contains two zinc ions bound at each subdomain (Figure 1b). The structural zinc cation bound at the catalytic domain is coordinated by interactions with the sulfur side chain atoms of four cysteines C96 (2.2 Å), C99 (2.2 Å), C102 (2.3 Å) and C110 (2.3 Å) (See Supporting Information Figure S8). The catalytic zinc cation, involved in substrate binding, is bound at the nucleotide binding subdomain via tetrahedral interactions (bond lengths in parenthesis for chain B) with C42(SG) (2.6 Å), C152(SG) (2.7 Å), T44(OG1) (2.1 Å) and H67(NE2) (2.6 Å) in chains B to D (Figure 1b). Another residue in close vicinity to the zinc binding site is E66, however its side-chain was not clearly visible at the given resolution. Interestingly, the involvement of a glutamate in zinc coordination was observed as an atypical feature in human liver χχ ADH (PDB entry 1TEH).[26] In agreement with the overoxidative activities of HeADH-II, the human enzyme catalyzes substrate oxidation of long-chain alcohols, and also *S*-hydroxymethyl-glutathione.[26]

Despite having different phylogenetic origins, similarities in the active sites of HeADH-II and human liver χχ ADH (E-value: $4.72E^{-09}$) and horse liver alcohol dehydrogenase (PDB entry 1QLH: E-value: $6.21E^{-07}$), which both carry out oxidative reactions were underlined by an enzyme template search using Profunc (http://www.ebi.ac.uk/thornton-srv/databases/ProFunc/; [26,28,31] (See Supporting Information).

HeADH-II and human liver χχ ADH share a low sequence identity of 28.9% (for 304/380 fit-ted residues), and a structural identity of 99.7% (Figure 2d). The local sequence identity (41 equivalenced residues) surrounding the three matched active site residues, increases to 48.8% with 20 identical and 8 similar neighboring active site residues, reflecting increased conservation in this region.

Direct coordination of E68 (human χχ ADH) has been proposed to represent a reaction intermediate that assists in product release and the water exchange step during catalysis. Accordingly, this glutamate is replaced by a coordinating water molecule in chain A of the human χχ ADH. The resolution of our data, however, was not sufficient to visualize water molecules.

The oxidation of long-chain alcohols, accommodated by a larger than usual active site in human liver χχ ADH, is suggested to occur via a catalytic mechanism similar to that of class I ADH that requires a significant decrease in the pKa of the alcohol substrate due to direct coordination with the zinc ion. As observed upon superposition of the two enzymes, HeADH-II also has a comparably large active site (Figure 1c). The catalytic mechanism of human liver χχ ADH is proposed to employ H47 (H67 in HeADH-II) as the catalytic base, with a double role also in NAD(H) binding. During the mechanism, a proton-relay pathway is suggested, involving transfer of the substrate's hydroxyl proton, with passage from inside the active site to the solvent. In class I ADHs, mutagenesis studies have shown that the proton relay is mediated by residues T48 (T44 in HeADH-II), the 2'-hydroxyl of the nicotinamide ribose in NAD(H), and the imidazole of His47, with the latter acting as the catalytic base in the reaction. Given the sequence and structural conservation of

analogous residues in HeADH-II, a similar mechanism may be implied.

Concerning horse liver ADH (HLADH), the zinc coordinating cysteines and histidine residues were matched (local sequence ID 35.7% over 41 equivalenced residues); a coordinating glutamate was not observed in the structure of HLADH, although the authors predicted its role computationally.[32] The authors also predicted the role of S48 (T44 in HeADH-II) in proton shuttling.

### *In silico* modelling and docking studies

To further study the catalytic properties of HeADH-II and integrate the information obtained with the apo-crystal structure, a model of the holo-form was created with MODELLER,[33] using as query the holo-form of the bacterial ADH from *Brucella melitensis* (BmADH, PDB entry 3MEQ) which has over 70% sequence identity. To complete the model, the zinc atoms were added and the cofactor, $NAD^+$, docked to the structure using autodock VINA software.[34] The resulting model, compared to the apo crystal structure, was only different in the position of three loops close to the active site (See Supporting Information, Figure S9).

As mentioned, ADHs normally exhibit very high enantioselectivities, closely related to the shape and size of the catalytic cleft which tends to display clearly differentiated small and large pockets. Such architecture favours efficient binding of just one stereoisomer (in the oxidative direction), and promotes the hydride transfer only to one face of the carbonyl molecule (in the reductive direction).[35] In contrast, HeADH-II appears to lack any enantiopreference with the tested substrates in either catalytic direction. Only a few wild-type ADHs have been found to have reduced enantiopreference[36,37] while protein engineering can lead to a less selective variants.[34,38,39] The catalytic cleft of HeADH-II appears to be symmetric, with undistinguishable pockets, unlike the majority of ADH structures reported (including that of BmADH).[34] To illustrate the differences in the catalytic cleft, RCR ((*R*)-selective carboxyl reductase from *Candida parapsilosis*) and TeSADH (non-enantioselective secondary alcohol dehydrogenase from *Thermoanaerobacter ethanolicum*) were compared to HeADH-II.[40,41] Despite a less than 30% of sequence homology (See Supporting Information, Figure S10A), the three enzymes exhibit a similar folding and a very similar architecture of the active site (See Supporting Information, Figure S10B), mainly differing in the size of their pockets (Figure 2A). In RCR, the two pockets are clearly distinguishable with a small pocket limited by F285 and W286. Upon mutation to alanine of either of those (F285A or W285A), the additional space causes the loss of enantioselectivity for (*R,S*)-2-phenyl-1-propanal.[42] The HeADH-II quasi symmetric catalytic site displays a I290 and a V291 which leave enough space in the upper pocket for bulky substituent (Figure 2B). In addition, T44 and specially the orientation of W91, extend the size of the other pocket, which mimics RCR and TeSADH. Both positions have been previously probed to investigate the stereoselectivity of HLADH.[38] Specifically, the presence of a phenylalanine in the corresponding W91 position, oriented towards the catalytic site, reduces the size of the pocket (See Supporting information, Figure S11). Notably, W91 in HeADH-II appeared to be quite static during the short MD simulation, staying parallel to the opening of the catalytic cleft, as in TeSADH.

Docking studies of HeADH-II with both (*R*)- and (*S*)-1-phenylethanol were performed; both enantiomers could be fitted in the active site with identical energies, very similar conformations, and catalytically plausible orientations (Figure 2B).

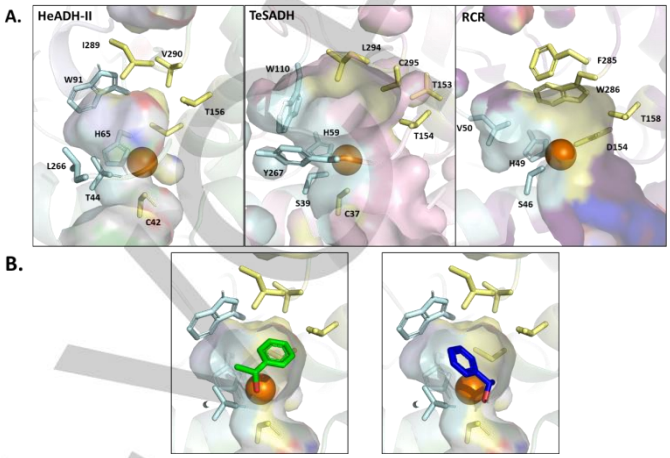


**Figure 2.** A) Comparison of the catalytic pockets of HeADH-II, TeSADH and RCR. The labelled residues which are defining each of the pockets are coloured in light cyan or yellow and their surface is shown. B) Detail of the docking of (*R*)- and (*S*)- 1-phenylethanol. The *S* enantiomer is shown in blue and the *R* in green. The docking energies obtained were -5.4 kcal/mol and -5.6 kcal/mol, respectively.

## Conclusion

We successfully characterized and applied a promiscuous halophilic ADH (HeADH-II) that can oxidize both alcohols and aldehydes to the corresponding carboxylic acid. Based on observations made between the crystal structure of HeADH-II, it shares structural characteristics with mammalian ADHs that also carry out oxidative reactions. Such structural similarities and common functional activities may imply a shared catalytic mechanism. This new enzyme demonstrated great activity and stability at high salt and polar solvent concentrations, usually employed for solubilizing organic compounds in water media. Enzymes derived from extremophiles, such as the halo-adapted bacterium *Halomonas elongata*, are particularly suitable for industrial processes thanks to their adaptation to harsher reaction environments. HeADH-II showed broad substrate specificity: different aromatic primary alcohols and aldehydes were fully converted to the final carboxylic acid. Moreover, the oxidation of racemic 1-phenylethanol to the corresponding ketone was obtained with good conversion, thus demonstrating enzyme versatility. Interestingly, no enantiopreference was observed. This uncommon characteristic could be explained by the symmetry observed in the catalytic pockets of HeADH-II which allows both (*R*)- and (*S*)-1-phenyl ethanol to fit as a mirror images in a catalytically plausible conformation. HeADH-II therefore can be included with only a few other examples in the list of non-stereoselective ADHs which could offer major ad-

vantages in hydrogen borrowing cascades for the synthesis of chiral amines from the racemic alcohols.[43]

To further optimize the process, in situ recycling of the cofactor was performed by adding a second enzyme (*Lp*NOX) that allowed the generation of a self-sustaining enzymatic system with the use of catalytic amounts of $NAD^+$. Unfortunately, the NADH-oxidase from *Lactobacillus pentosus* (*Lp*NOX) was found to be unstable at prolonged reaction times, so fed-batch experiments were carried out to obtain a two-step transformation with almost complete conversion. Further applications particularly focused on the enzymatic preparation of perillartine (deriving from the condensation of aldehydes with hydroxylamine) were performed. This reaction proceeds at room temperature and under the atmospheric pressures. Using an $NAD^+$ regenerating system, catalytic amount of the cofactor could be employed. As the only by-product is water, this system can be considered sustainable and applicable for the preparation of natural food ingredients.

## Experimental Section

### General

NMR spectra were recorded on a Varian Gemini 300 MHz spectrometer using the residual signal of the deuter-ated solvent as internal standard. $^1H$ chemical shifts ($\delta$) are expressed in ppm, and coupling constants ($J$) in hertz (Hz). Merck Silica gel 60 F254 plates were used for analytical TLC; flash column chromatography was performed on Merck Silica gel (200–400 mesh).

### Chemicals

All reagents and solvents were obtained from commercial suppliers and were used without further purification.

### Cloning, expression and purification

The synthetic gene encoding for HeADH-II from *Halomonas elongata*, directly cloned into vector pET-28b(+) was purchased from BaseClear. The gene, optimized for the expression in *E. coli*, presented an *N*-terminal his-tag. The resulting pET28b-HeADH-II was transformed into chemically competent *E. coli* BL21 (DE3) pLYsS for heterologous expression. Plates of *E. coli* BL21 (DE3) pLYsS pET28b-HeADH-II were grown overnight at 37 °C in LB-agar medium supplemented with 25 µg/mL kanamycin and 35 µg/mL chloramphenicol. 200 mL of autoinduction medium: 10 g/L N-Z amine, 5 g/L yeast extract, 50 mL $KH_2PO_4$ 1 M, 50 mL $K_2HPO_4$ 1 M, 25 mL $(NH_4)_2SO_4$ 1 M, 2 mL $MgSO_4$ 1 M, 2 mL trace element solution ($FeSO_4$ 50 mM, $CaCl_2$ 20 mM, $MnCl_2$ 10 mM, $ZnSO_4$ 10 Mm, $CoCl_2$ 2 mM, $CuCl_2$ 2 mM, $NiCl_2$ 2 mM, HCl 60 mM, $NaMoO_4$ 2 mM, $H_3BO_3$ 2 mM), 20 mL 5052 solution (250 g/L glycerol, 25 g/L glucose, 100 g/L α-lactose), 25 µg/mL kanamycin, 35 µg/mL chloramphenicol) were inoculated with a single colony. The cultures were further incubated for 16 h at 37 °C, 120 rpm. Cells were then harvested by centrifugation (15 min, 5000 rpm, 4 °C), washed once with deionized water and stored at -20 °C; 10 g of pellet were resuspended in 50 mL loading buffer (Tris-HCl 100 mM pH 8.0, imidazole 20 mM, NaCl 100 mM) and sonicated (6 cycles of 2 min each, in ice, with 1 min interval). Cell debris were harvested by centrifugation (45 min, 15000 rpm, 4 °C). Chromatography was performed using ÄKTA Purifier (GE Healthcare) with a 1 mL column HisTrapTM FF (GE Healthcare) pre-loaded with $NiSO_4$ (100 mM). Briefly, the column was equilibrated with loading buffer and the filtered crude extract loaded; column was then washed with loading buffer; finally, the adsorbed enzyme was eluted with elution buffer (Tris-HCl 100 mM pH 8.0, imidazole 250 mM, NaCl 100 mM).

Crude extract, pellet and pure protein were analyzed by SDS-PAGE (See Supporting information, Figure S4). The fractions showing the presence of a band of the expected size (38 kDa) were pooled, dialyzed against Tris-HCl buffer 100 mM, pH 8.0 and stored at 4 °C. Typically, starting from 10 g of wet cell paste, it was possible to obtain 5 mg of pure protein.

The plasmid pET28a(+) containing the gene encoding for *Lp*NOX was kindly provided by Prof. Sieber (University of München). The enzyme was expressed and purified as previously reported.[44]

Crude extract, pellet and pure protein were analyzed by SDS-PAGE (See Supporting information, Figure S5). The fractions showing the presence of a band of the expected size (52 kDa) were pooled, dialyzed against Tris-HCl buffer 100 mM, pH 8.0 and stored at 4 °C. Typically, starting from 2 g of wet cell paste, it was possible to obtain 10 mg of pure protein.

### HeADH-II activity assays

Activity measurements were performed spectrophotometrically at 340 nm by determining the formation or depletion of NADH at 25 °C in a half-microcuvette (total volume 1 mL) for 2 min. One unit (U) of activity is defined as the amount of enzyme which catalyzes the consumption of 1 µmol of $NAD^+$/NADH per minute under reference conditions, namely 1 mM $NAD^+$/NADH, 4 mM cinnamyl alcohol/cinnamaldehyde, correct amount of HeADH-II in Tris-HCl 100 mM, pH 8.0. Specific activity was 3 U/mg and 2.8 U/mg, respectively.

### *Lp*NOX activity assay

Activity measurements were performed spectrophotometrically at 340 nm by determining the depletion of NADH at 25 °C in a half-microcuvette (total volume 1 mL) for 2 min. One unit (U) of activity is defined as the amount of enzyme which catalyzes the consumption of 1 µmol of NADH per minute under reference conditions, namely 1 mM NADH, correct amount of *Lp*NOX in Tris-HCl, 100 mM, pH 8.0. Specific activity was 50 U/mg.

### Biotransformations

Molar conversion and enantioselectivity towards different aromatic alcohols and aldehydes were determined by performing biotransformations at 20-mg scale, using an enzyme-coupled system (*Lp*NOX) for cofactor recycling. Oxidations were carried out in 10-mL screw-capped test tubes with HeADH-II (1

U/mL), *Lp*NOX (10 U/mL), $NAD^+$ (0.1 mM), FAD (0.1 mM), substrate (20 mM), DMSO (20% *v/v*) suspended in Tris-HCl buffer 100 mM pH 8.0. To determining conversion of the enzymatic reactions 100 µL aliquots were quenched with HCl 0.1 M at different reaction times and extracted with 100 µL of AcOEt for TLC (*n*-Hexane/AcOEt 9:1). Samples, after evaporation, were resuspended in the mobile phase for HPLC analysis (See Supporting Information).

**One-pot reaction for the preparation of aldoximes**

One-pot biotransformations were carried out at 20-mg scale using 20 mM alcohol as substrate in DMSO (15% *v/v*), $NH_2OH{\cdot}HCl$ (24 mM), 0.1 mM $NAD^+$, 0.1 mM FAD, HeADH-II (1 U/mL), *Lp*NOX (10 U/mL), in Tris-HCl buffer 100 mM, pH 8.0 at 30 °C. 150 µL aliquots were extracted with AcOEt at different reaction times and analyzed by gas-chromatography (See Supporting Information).

## Acknowledgements ((optional))

This project was supported by the European Union's Horizon 2020 research and innovation programme under the Marie Skłodowska-Curie grant agreement no. 792804 AROMAs-FLOW (M. L. C.). L. J. G. was supported by Linea 2 Università degli Studi di Milano funding.

**Keywords:** Alcohol dehydrogenase • *Halomonas elongata* • Overoxidation • Biocatalysis • Aldoxyme synthesis

[1] D. Monti, G. Ottolina, G. Carrea, S. Riva, *Chem. Rev.* **2011**, *111*, 4111–4140.

[2] Y. G. Zheng, H. H. Yin, D. F. Yu, X. Chen, X. L. Tang, X. J. Zhang, Y. P. Xue, Y. J. Wang, Z. Q. Liu, *Appl. Microbiol. Biotechnol.* **2017**, *101*, 987–1001.

[3] M. L. Contente, F. Paradisi, *Nat. Catal.* **2018**, *1*, 452-459.

[4] J. An, Y. Nie, Y. Xu, *Crit. Rev. Biotechnol*. **2019**, 366–379.

[5] J. Liu, S. Wu, Z. Li, *Curr. Opin. Chem. Biol*. **2018**, *43*,77–86.

[6] L. P. Olson, J. Luo, O. Almarsson, T. C. Bruice, *Biochemistry* **1996**, *35*, 9782–9791.

[7] C. Wuensch, H. Lechner, S. M. Glueck, K. Zangger, M. Hall, K. Faber, *ChemCatChem* **2013**, *5*, 1744–1748.

[8] J. Dong, E. Fernandez-Fueyo, F. Hollmann, C. E. Paul, M. Pesic, S. Schmidt, Y. Wang, S. Younes, W. Zhang., *Angew. Chem. Int. Ed.* **2018**, *57*, 9238–9261.

[9] P. Könst, H. Merkens, S. Kara, S. Kochius, A. Vogel, R. Zuhse, D. Holtmann, I. W. C. E. Arends, Hollmann F., *Angew. Chem. Int. Ed.* **2012**, *51*, 9914–9917.

[10]D. Romano, R. Villa, F. Molinari, *ChemCatChem* **2012**, *4*, 739–749.

[11]D. Romano, M. Contente, T. Granato, W. Remelli, P. Zambelli, F. Molinari, *Monatsh. Chem.* **2013**, *14*, 735–737.

[12]A. Trincone, *Mar. Drugs* **2011**, *9*, 478–499.

[13]D. Alsafadi, S. Alsalman, F. Paradisi, *Org. Biomol. Chem.* **2017**, *15*, 9169–9175.

[14]S. W. Grötzinger, R. Karan, E. Strillinger, S. Bader, A. Frank, I. S. Al Rowaihi, A. Akal, W. Wackerow, J. A. Archer, M. Rueping, D. Weuster-Botz, M. Groll, J. Eppinger, S. T. Arold, *ACS Chem. Biol.* **2018**, *13*, 161−170.

[15]A. L. Akal, R. Karan, A. Hohl, I. Alam, M. Vogler, S. W. Grötzinger, J. Eppinger, M. Rueping, *FEBS Open Bio* **2019**, *9*, 194–205.

[16]L. Cerioli, M. Planchestainer, J. Cassidy, D. Tessaro, F. Paradisi, *J. Mol. Catal. B: Enzym.* **2015**, *120*, 141–150.

[17]M. Planchestainer, M. L. Contente, J. Cassidy, F. Molinari, L. Tamborini, F. Paradisi, *Green Chem.* **2017**, *9*, 372–375.

[18]D. Roura-Padrosa, V. De Vitis, M. L. Contente, F. Molinari, F. Paradisi, *Catalysts* **2019**, *9*, 232-242.

[19]M. L. Contente, F. Dall'Oglio, L. Tamborini, F. Molinari, F. Paradisi, *ChemCatChem* **2017**, *9*, 3843-3848.

[20]S. N. Ashakirin, M. Tripathy, U. K. Patil, A. B. A. Majeed, *Int J. Pharm. Sci.* **2017**, *8*, 2333-2340.

[21]A. A. Koesoema, D. M. Standley, T. Senda, T. Matsuda, *Appl. Microbiol. Biotechnol.* **2020**, *104*, 2897–2909

[22]J. D. Zhang, Z. M. Cui, X. J. Fan, H. L. Wu, H. H. Chang, *Bioprocess Biosyst. Eng.* **2016**, *39*, 603-611.

[23]P. Zambelli, A. Pinto, D. Romano, E. Crotti, P. Conti, L. Tamborini, R. Villa, F. Molinari, *Green Chem.* **2012**, *14*, 2158-2161.

[24]R. K. Saini, S. Sravan Kumar, S. Priyanka, K. Kamireddy, P. Giridhar in Biotechnological Production of Natural Ingredients for Food Industry, 1st ed, Bentham Science Publisher Sharjah, **2016**, pp 21-59.

[25]E. Krissinel, K. Henrick, *J. Mol. Biol.* **2007**, 372, 774-797.

[26]Z. N. Yang, W. F. Bosron, T. D. Hurley, *J. Mol. Biol.* **1997**, *265*, 330–343.

[27]E. F. Pettersen, T. D. Goddard, C. C. Huang, G. S. Couch, D. M. Greenblatt, E. C. Meng, T. E. Ferrin, *J. Comput Chem.* **2004**, *25*, 1605-1612.

[28]S. Ramaswamy, D. H. Park, B. V. Plapp, *Biochemistry*, **1999**, *38*, 13951–13959.

[29]L. Holm, *Bioinformatics* **2019**, *35*, 5326-5327.

[30]S. Y. Jun, A. M. Walker, H. Kim, J. Ralph, W. Vermerris, S. E. Sattler, C. Kang, *Plant Physiol.* **2017**, *174*, 2128–2145.

[31]R. A. Laskowski, J. D. Watson, J. M. Thornton, *Nucleic Acids Res.* **2005**, *33*(Web Server issue), W89–W93.

[32]L. P. Olson, J. Luo, Ö. Almarsson, T. C. Bruice, *Biochemistry* **1996**, *35*, 9782–9791.

[33]B. Webb B, A. Sali, *Curr. Protoc. Bioinformatics* **2016**, *54*, 5.6.1-5.6.37.

[34]M. A. Maria-Solano, A. Romero-Rivera, S. Osuna, *Org. Biomol. Chem.* **2017**, *15*, 4122-4129.

[35]F. M. Dickinson, K. Dalziel, *Nature* **1967**, *214*, 31–33.

[36]I. Lavandera, A. Kern, V. Resch, B. Ferreira-Silva, A. Glieder, W. M. F. Fabian, S. de Wildeman, W. Kroutil, *Org. Lett.* **2008**, *10*, 2155–2158.

[37]F. Chen, Y. Liu, G. Zheng, J. Xu, *ChemCatChem* **2015**, *7*, 3838-3841.

[38]K. Kim, B. V. Plapp, *Chem-Biol Interact.* **2017**, *276*, 77–87.

[39]J. M. Patel, M. M. Musa, L. Rodriguez, D. A. Sutton, V. V. Popik, R. S. Phillips, *Org. Biomol. Chem.* **2014**, *12*, 5905–5910.

[40]D. S. Burdette, C. Vieille, J. G. Zeikus, *Biochem. J.* **1996**, *316*, 115–122.

[41]Y. Nie, Y. Xu, X. Q. Mu, *Org. Process Res. Dev.* **2004**, *8*, 246–251.

[42]S. Wang, Y. Nie, Y. Xu, R. Zhang, T. P. Ko, C. H. Huang, H. C. Chan, R. T. Guo, R. Xiao, *Chem. Commun.* **2014**, *50*, 7770–7772.

[43]F. G. Mutti, T. Knaus, N. S. Scrutton, M. Breuer, N. J. Turner, *Science* **2015**, *349*, 1525–1529.

[44]C. Nowak, B. Beer, A. Pick, T. Roth, P. Lommes, V. Sieber, *Front. Microbiol.* **2015**, *6*, 957-965.

## Entry for the Table of Contents

Insert graphic for Table of Contents here. ((Please ensure your graphic is in **one** of following formats))

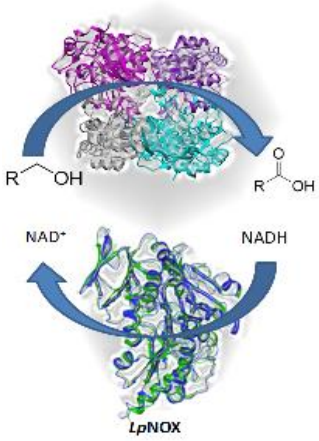


An unusual alcohol dehydrogenase has been identified from the halo-adapted bacterium *H. elongata.* HeADH-II shows a great stability to polar solvents and high salt concentration as well as uncommon characteristics as the lacking of enantiopreference and the capability of overoxidizing alcohols to carboxylic acids. To increase the process yields and allowing the cofactor recycling HeADH-II was coupled with a NADH-oxidase from *L. pentosus* (*Lp*NOX).

Institute and/or researcher Twitter usernames: ((optional))